JACS
JOURNAL OF THE AMERICAN CHEMICAL SOCIETY
Article
pubs.acs.org/JACS

Picosecond Binding of the His Ligand to Four-Coordinate Heme in Cytochrome *c*′: A One-Way Gate for Releasing Proximal NO

Byung-Kuk Yoo,[†,§] Isabelle Lamarre,[†] Jean-Louis Martin,[†] Colin R. Andrew,[‡] and Michel Negrerie*[,†]

[†]Laboratoire d'Optique et Biosciences, INSERM, Ecole Polytechnique, 91128 Palaiseau Cedex, France
[‡]Department of Chemistry and Biochemistry, Eastern Oregon University, La Grande, Oregon 97850, United States

ABSTRACT: We provide a direct demonstration of a "kinetic trap" mechanism in the proximal 5-coordinate heme-nitrosyl complex (5c-NO) of cytochrome *c*′ from *Alcaligenes xylosoxidans* (AXCP) in which picosecond rebinding of the endogenous His ligand following heme-NO dissociation acts as a one-way gate for the release of proximal NO into solution. This demonstration is based upon picosecond transient absorption changes following NO photodissociation of the proximal 5c-NO AXCP complex. We have determined the absolute transient absorption spectrum of 4-coordinate ferrous heme to which NO rebinds with a time constant τ_{NO} = 7 ps (k_{NO} = 1.4 × 10^{11} s^{-1}) and shown that rebinding of the proximal histidine to the 4-coordinate heme takes place with a time constant τ_{His} = 100 ± 10 ps (k_{His} = 10^{10} s^{-1}) after the release of NO from the proximal heme pocket. This rapid His reattachment acts as a one-way gate for releasing proximal NO by precluding direct proximal NO rebinding once it has left the proximal heme pocket and requiring NO rebinding from solution to proceed via the distal heme face.

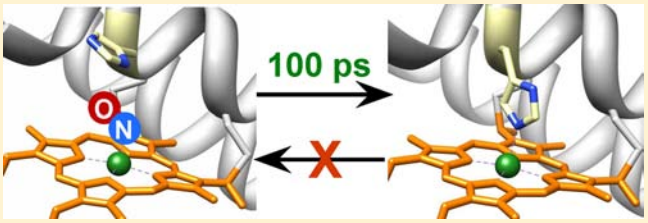

INTRODUCTION

Cytochromes *c*′ (Cyts *c*′) are *c*-type heme proteins present in many nitrogen-fixing, denitrifying, and photosynthetic bacteria.[1] Unlike mitochondrial cytochrome *c*, bacterial Cyts *c*′ are usually homodimeric, with each four α-helical subunit harboring a mono-His liganded heme in which the distal coordination site remains vacant in the absence of diatomic ligands. While Cyts *c*′ have been studied for 40 years, their physiological function and exact biochemical role(s) are unresolved. Apart from the general functions based on the redox properties of *c*-type heme,[2] studies have focused on their possible protective role against the toxicity of NO in bacteria as either NO reductases or NO transporters. The Cyt *c*′ from the bacteria *Rhodobacter capsulatus* (RCCP) has been shown to protect bacteria against exogenous NO toxicity.[3,4] The wild-type RC strain was further shown to produce N_2O when grown in the presence of NO, contrary to the MC111 mutant which does not synthesize Cyt *c*′, suggesting that RCCP is involved in reductase activity.[4] However, a direct NO-reductase activity was not demonstrated *in vitro* for any purified Cyt *c*′, and its role as a NO-transporter coupled to a NO-reductase has been proposed for the two species *Chromotium vinosum*[5] and *Rhodobacter sphaeroides*.[6]

Cyt *c*′ from *Alcaligenes xylosoxidans* (AXCP) exhibits unusual heme-NO reactivity. Whereas heme proteins generally form 6-coordinate complexes with NO, AXCP becomes 5c-NO, like the NO-receptor soluble guanylate cyclase (sGC).[7] The cleavage of the proximal Fe-His bond triggers the catalytic activity in sGC, but the exact role of the proximal bond breaking and formation of a proximal 5c-NO AXCP is still in question.[8] Importantly, the crystal structure of 5c-NO AXCP has revealed that NO ligand resides at the proximal heme side in place of the endogenous proximal His120 ligand,[9,10] whereas CO forms a 6-coordinate heme complex at the vacant distal side. The binding of NO to the unliganded AXCP first occurs to the empty distal side of the heme,[8] forming a transient 6c-NO complex. Subsequent 6c-NO to 5c-NO conversion (cleavage of the Fe-His bond by trans effect) results from a weakening of the axial Fe-His bond caused by the trans-coordination of NO,[11,12] a property shared by bacterial NO-sensors[13] and by the NO-receptor guanylate cyclase.[7,14] However, in AXCP the breaking of the Fe-His bond allows the binding of a second NO molecule at the proximal side to form a dinitrosyl [6c-$(NO)_2$], which quickly loses the original distal NO, leading to the proximal 5c-NO product. The formation of the stable 5c-NO proximal heme thus occurs through two steps which are NO concentration dependent, via the 6c-NO,[15] distal 5c-NO, and a heme-dinitrosyl intermediates.[8,10] Although the crystal structure of 5c-NO sGC has yet to be determined, EPR spectroscopic and kinetic data suggest that NO might also bind proximally in 5c-NO sGC.[14,16] Proximal versus distal binding represents a mode of heme ligand selectivity that must be important to the proposed NO-binding role of AXCP.

Factors affecting the release of NO from 5c-NO complexes are particularly important in the context of the proposed AXCP role as NO-carrier. For most heme-nitrosyl protein complexes, after the dissociation (thermal or photoinduced) of NO from the iron has occurred, its geminate rebinding takes place in a multiphasic manner in the picosecond[17] or in the nanosecond

Received: December 12, 2012
Published: February 1, 2013

   dx.doi.org/10.1021/ja312140f | *J. Am. Chem. Soc.* 2013, 135, 3248−3254

time range[18] according to the internal energy barriers which control NO dynamics. For sGC the NO geminate recombination to the 4-c heme after dissociation was revealed to be monoexponential (time constant of 7.5 ps; 97%).[7,19] We found in a previous study[20] that after NO dissociation the structure of the proximal heme pocket of AXCP confines NO close to the iron so that an ultrafast and monoexponential geminate rebinding similarly occurs to the proximal heme side with a high yield (time constant of 7 ps; 99%) before the proximal histidine rebinding can occur. The His rebinding process was not detected because of the uncertainty about its time constant and because of the very small amplitude of the transient spectrum remaining after NO geminate rebinding.

In the present work we identified the process which represents ∼1% of the dissociated AXCP population and for which NO does not rebind. We aimed at identifying its coordination state and dynamics after NO dissociation. Indeed, the time scale of His rebinding relative to that of proximal 5c-NO geminate recombination has strong implications for the mechanism of NO proximal release and rebinding in AXCP and thus its reactivity. Previous experiments indicated that the proximal His120 reattachment is faster than 5 ms and was hypothesized to compete with NO rebinding either in a geminate manner or in a bimolecular manner from the solution, in both cases the dissociated proximal histidine playing a central role in a proposed "kinetic trap" mechanism.[21] However, the time resolution used was not high enough to allow a conclusion to be made. In the present work, ultrafast time-resolved spectroscopy in picosecond and nanosecond time windows with probing in a wide spectral range was mandatory to detect the formation of transient 5c-His heme immediately after NO dissociation from the iron. We have recorded the transient absorption spectra of AXCP after photodissociation of NO to detect simultaneously the evolution of the 5c-NO, 5c-His, and 4c heme species. In such experiments, the thermal dissociation of NO previously bound to the heme is simulated by photodissociation (50-fs laser pulse), allowing us to probe the heme state and dynamics as a function of time from the nonequilibrium dissociated AXCP, with NO still moving within the protein core. Here, we identified the 4c heme transient spectrum and the fast rebinding process of proximal His to the 4-coordinate heme. Transient absorption spectra of photodissociated 6c-NO and 6c-CO AXCP complexes with distal gas ligands were also recorded to help distinguish distal from proximal ligand dynamics.

EXPERIMENTAL SECTION

Preparation of the Samples. AXCP was purified as previously described.[22,23] The protein was kept frozen (−80 °C) in MES buffer (pH 6) at 0.47 mM, thawed immediately before the spectroscopic measurements, and diluted to the working concentration. The solution of ferric AXCP (100 μL, 75 μM) was put in a 1-mm optical path length quartz cell sealed with a rubber stopper and degassed by means of four successive cycles of vacuum and purging with pure argon. The heme iron was reduced by the addition of 10 μL of degassed sodium ascorbate solution (5 mM final concentration). For preparing the 5-c and 6-c NO-liganded AXCP, gas-phase 100% or 0.1% NO diluted in N_2 was directly introduced into the spectroscopic cell (2 mM and 2 μM of NO in the aqueous phase, respectively). To obtain the 100% CO-bound form, AXCP was equilibrated with 1 atm of CO gas (∼1 mM in aqueous phase). Equilibrium spectra were recorded at each step for monitoring the evolution of Soret band and the coordination state. The absorbance of the sample was in the range 0.7−1 at the Soret maximum for a 1-mm path length.

Time-Resolved Absorption Spectroscopy. Femtosecond absorption spectroscopy was peformed with the pump−probe laser system previously described.[24] The photodissociation of NO was achieved with an excitation pulse at 564 nm, in the Q-band absorption, whose duration was ∼40 fs with a repetition rate of 30 Hz. The transient Soret absorption was recorded with a variable delay between pump and probe pulses. The optical path length of the cell was 1 mm. The sample temperature was 18 °C during all measurements. Transient spectra were recorded with a CCD detector simultaneously to kinetics as time−wavelength matrix data. Transient spectral analysis of the data was performed by singular value decomposition (SVD)[24,25] of the time−wavelength matrix such that all spectral components were identified in the multiple time windows ranging from 20 ps to 5 ns. Up to 40 scans were recorded and averaged with a dwell time of 2 s at each point. The SVD kinetic components associated with each SVD spectral component were fit to a sum of a minimum number of exponentials.

Calculation of the 4-Coordinate Heme Spectrum. The absorption spectrum of the four-coordinate ferrous heme was obtained by subtracting the weighted spectrum of 5c-NO AXCP measured before photodissociation (negative time) from that measured at +10 ps after dissociation. This time delay was chosen to minimize the presence of excited states, which decay with a 4-ps time constant, but maximizing the population of 4c-heme and minimizing the 5c-His population due to His rebinding with a larger time constant. The weighting coefficient depends upon the delay and was calculated from the relation $C_p(t) = \Delta A_{obs}(t)/\Delta\varepsilon l$, where $C_p(t)$ is the photoproduct concentration at a given delay, $\Delta A_{obs}(t)$ is the difference of absorbance at time t, $\Delta\varepsilon$ is the difference of absorption coefficients of the product and initial species, and l = 0.1 cm is the optical path length. It is necessary to make a starting assumption for ε of 4c-heme. Since we have observed almost symmetric bleaching and induced absorption intensities in difference transient spectra after 5c-NO photodissociation for two proteins yielding a 4c-heme, AXCP, and sGC,[7] we assumed that ε is of same order of magnitude for 4c- and 5c-NO. Starting with the value $\varepsilon = 90 \times 10^3$ $mol^{-1}\cdot L\cdot cm^{-1}$, we iteratively determined the coefficient 0.07 ± 0.01; a higher value resulted in negative features in the absolute 4c-heme spectrum, whereas a lower value gave rise to a shoulder due to 5c-NO heme. The spectrum of the 4c ferrous heme was therefore obtained as follows:

$$\text{spectrum(4c-heme)} = \text{spectrum(+10 ps)} - 0.93 \times \text{spectrum(−5 ps)}$$

RESULTS

The equilibrium spectra of unliganded ferrous AXCP and liganded with 100% NO, 0.1% NO, and 100% CO are displayed together with the corresponding difference spectra (Figure 1). The split Soret band of unliganded ferrous AXCP (425, 435 nm) has been shown to be due to a single type of 5c ferrous heme. Upon reaction of AXCP with 100% NO, a characteristic Soret maximum at 396 nm is observed (Figure 1A) corresponding to 5c-NO heme.[20] The proximal 5c-NO AXCP species is formed via a 6c-NO intermediate, whose lifetime is considerably increased at low NO concentration since the conversion of 6c-NO to 5c-NO is [NO] dependent.[8,26] We thus used 0.1% NO in gas phase (2 μM in aqueous phase) to obtain the 6c-NO steady-state species. The maximum of the Soret envelope at 420 nm (Figure 1B) is due to the mixture of ∼10% 6c-NO liganded intermediate[8,26] stabilized at low NO concentration and ∼90% 5c-His unliganded AXCP. The presence of the latter has no effect on the subsequent transient measurements. The 6c-CO AXCP complex (Figure 1C) possesses a Soret at 418 nm with high absorption coefficient.[12]

dx.doi.org/10.1021/ja312140f | J. Am. Chem. Soc. 2013, 135, 3248−3254

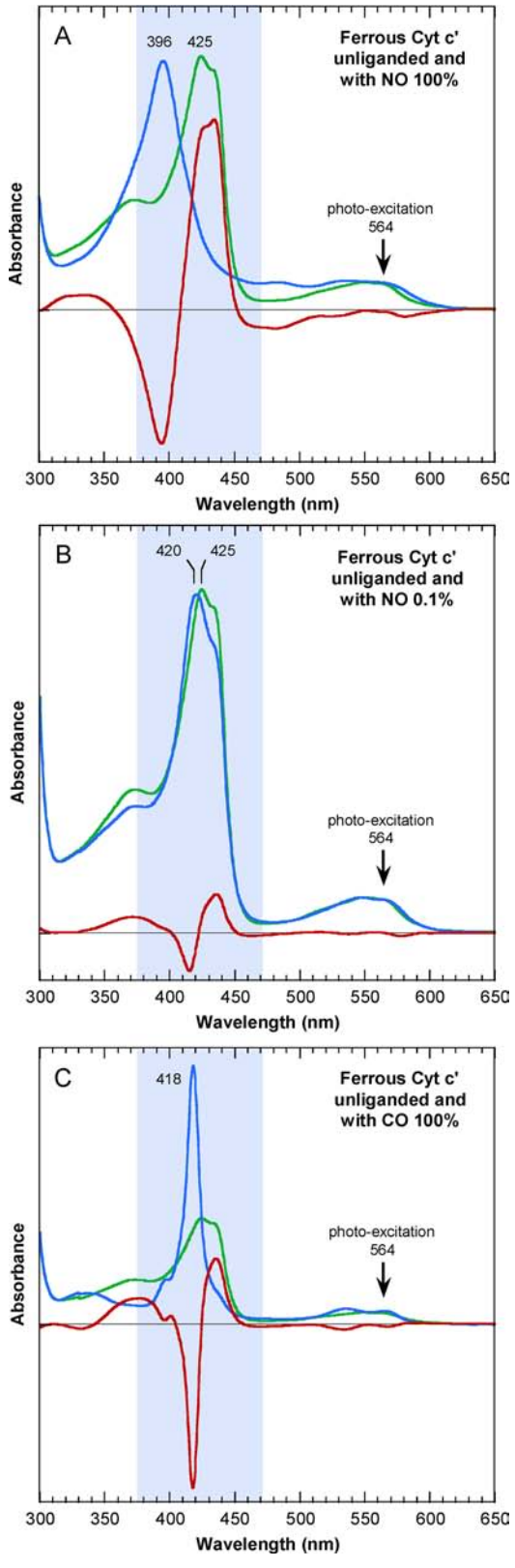

Figure 1. Equilibrium absorption spectra of unliganded (green) and liganded (blue) AXCP with corresponding difference spectra (red). (A) Incubation with 100% NO to generate a 5c-NO bound end product. (B) Incubation with 0.1% NO generating ~10% 6c-NO bound species and ~90% 5c-His species. (C) The 100% CO-bound form. The colored area indicates the Soret spectral range probed by time-resolved spectroscopy.

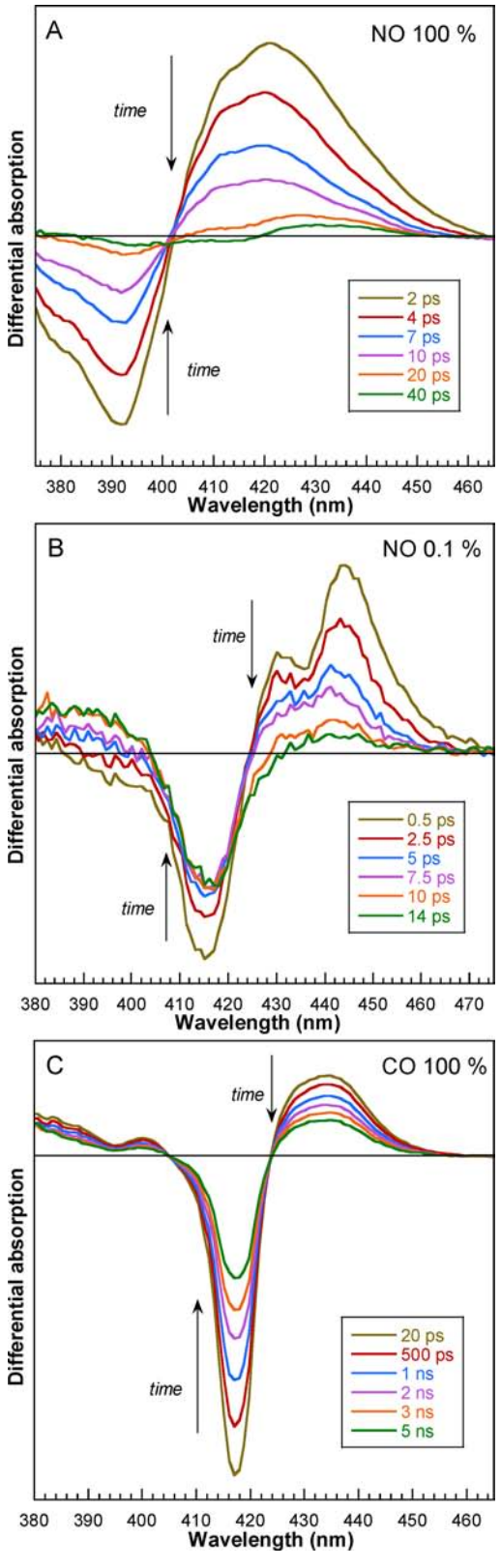

Figure 2. Raw transient spectra at different selected time delays after ligand photodissociation from ferrous AXCP in the presence of (A) 100% NO, (B) 0.1% NO, or (C) 100% CO.

Transient Species in 5c-NO AXCP. The kinetics of the Soret band were recorded after ligand photodissociation. The raw difference transient absorption spectra at various time delays are shown in Figure 2. For 5c-NO AXCP (100% NO),

dx.doi.org/10.1021/ja312140f | J. Am. Chem. Soc. 2013, 135, 3248−3254

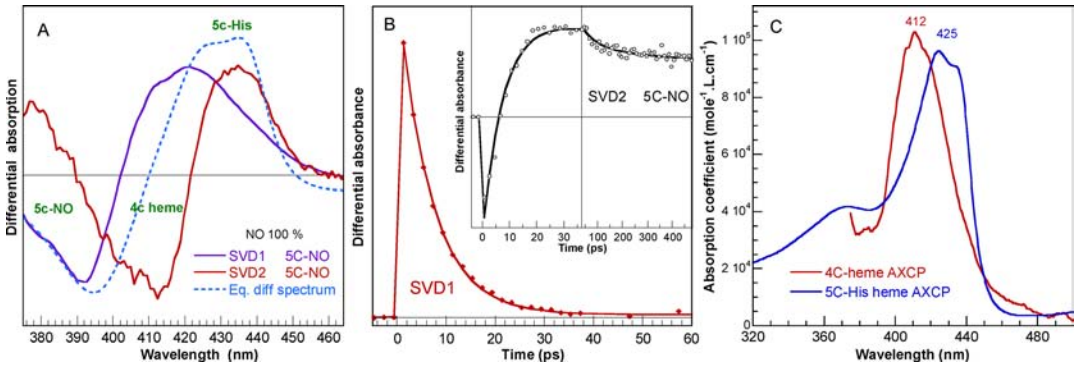

Figure 3. Identification of the transient components in 5c-NO AXCP. (A) Normalized spectral components (solid lines) obtained from SVD analysis of raw data from 5c-NO AXCP, compared with the equilibrium difference spectra "unliganded − 5c-NO liganded". The species involved are labeled in green. (B) Kinetic components from SVD analysis describing the evolution of the spectral components in panel A. Fit parameters are in Table 1. (C) Calculated transient spectrum of 4c heme compared with the 5c-His equilibrium spectrum.

Table 1. Time Constants Obtained from Fitting the Kinetics

	geminate rebinding	histidine rebinding	constant
AXCP state	τ_{gem} $(A_1)^a$	τ_{His} $(A_2)^a$	$A_3{}^a$
5c-NO	7 ps (*98.5*)	100 ps (*1.5*)	–
6c-NO	52 ps (*43*)	–	57
6c-CO	218 ps (*4*)	–	38
	1.9 ns (*58*)		

[a]Relative proportion ($A_i/\sum\Sigma A_i$ in %) of the component (the excited states relaxation are not taken into account).

the bleaching centered at 392 nm is due to the dissociation of the 5c-NO (Figure 2A) and the broad induced absorption is due to the appearance of 4c-heme AXCP. Both features simultaneously decrease in intensity from 2 to 15 ps because of NO geminate rebinding. A small contribution of induced absorption at 430 nm starts to appear from 15 ps, inducing a shift of the absorption maximum with respect to the spectra at shorter time, showing that two processes take place, which are quantitatively analyzed and identified below.

To obtain 6c-NO AXCP, we have used a very low NO concentration (0.1% NO in gas phase, yielding [NO] = 2 μM in solution) and a high stoichiometric ratio [AXCP]/[NO] = 37. In these conditions the formation of 5c-NO, which depends upon NO concentration, is extremely slow.The signal-to-noise ratio is lower due to the low concentration of NO which results in only <10% of the protein with NO bound (Figure 1B). Transient spectra following dissociation of NO from 6c-NO AXCP show a very different pattern compared to 5c-NO. The bleaching centered at 415 nm corresponds to the disappearance of 6c-NO species and partially recovers until 14 ps (Figure 2B) and a minor bleaching centered at 395 nm is due to 5c-NO, not detectable in the equilibrium spectrum. The isosbestic point moves from 386 nm at 0.5 ps to 404 nm at 14 ps, and the second is displaced from 425 to 432 nm in the same time range. This is due to the simultaneous rebinding of 5c-NO and 6c-NO. Thus, the induced absorption at early time (1−4 ps) is a mixture of 4c- and 5c-His heme, to which NO rebinds with different time constants. Because NO rebinds rapidly to the 4c-heme,[20] at longer time delay (>14 ps) the transient difference spectra are due only to the dissociation of 6c-NO. The raw transient spectra at successive time delays up to 5 ns after photolysis of CO are displayed in Figure 2C. The maximum of induced absorption centered at 434 nm and the minimum of bleaching at 417 nm clearly decrease simultaneously without any shift until 5 ns. These extrema are the same as in equilibrium difference spectra (Figure 1C) and the two isosbestic points at 405 and 424 nm do not shift, showing that only one process takes place. The kinetics of these transient spectra are only due to the rebinding of CO to AXCP, a process which does not occur in the ps-ns time range for Mb and with very low amplitude for sGC.[19]

To separate the contributions from the different transient species and their associated kinetics after photodissociation of NO from 5c-NO AXCP, we performed SVD analysis of the raw data matrix.[24] Two SVD spectral components are obtained and are remarkably different from the equilibrium difference spectrum of 5c-His *minus* 5c-NO AXCP (Figure 3A). The first spectral component, SVD1 having the highest singular value has overall similar shape with initial raw transient spectra (Figure 2A) is the contribution of geminate rebinding of NO to 4c AXCP. The characteristic bleaching at 392 nm is due to 5c-NO disappearance and the broad induced absorption, centered at 421 nm, is thus assigned to 4c heme.[7,20,27] Indeed, this broad induced absorption does not match that of equilibrium difference spectra, which is centered at 430 nm and is due to 5c-His heme. On the contrary, the absorption part of the second spectral component SVD2 (Figure 3A) centered at 435 nm matches the "red" edge (440−460 nm) of the equilibrium difference spectra and was thus assigned to the 5c-His species formed from the 4c-heme after His rebinding. Thus, transient absorption changes following photolysis of the proximal 5c-NO adduct detect proximal NO rebinding as well as His rebinding to 4c-heme.

Rate of His Rebinding after NO Dissociation. The two SVD kinetic components associated with SVD transient spectra were fitted (Figure 3B) to a sum of exponential functions. However, a monoexponential function with time constant of τ_1 = 7 ± 0.5 ps was sufficient in the case of SVD1, due to the geminate rebinding of NO to the 4c heme, with same time constant as already measured for other 5c-NO heme proteins[7,27] and isolated heme.[28] The kinetics associated with SVD2 (Figure 3B, inset) were fitted with a sum of two exponential functions: a 7-ps contribution from NO recombination and a slower exponential decay with τ_2 = 100 ± 10 ps with small overall amplitude (A_2 = 1.5 ± 0.5% calculated with the approximation that 4c- and 5c-His hemes have similar absorption coefficients, see below) yielding k_{His} = 10^{10} s^{-1} for proximal His rebinding to the 4c heme in AXCP after NO release from the heme pocket. It must be noted that the two

dx.doi.org/10.1021/ja312140f | J. Am. Chem. Soc. 2013, 135, 3248−3254

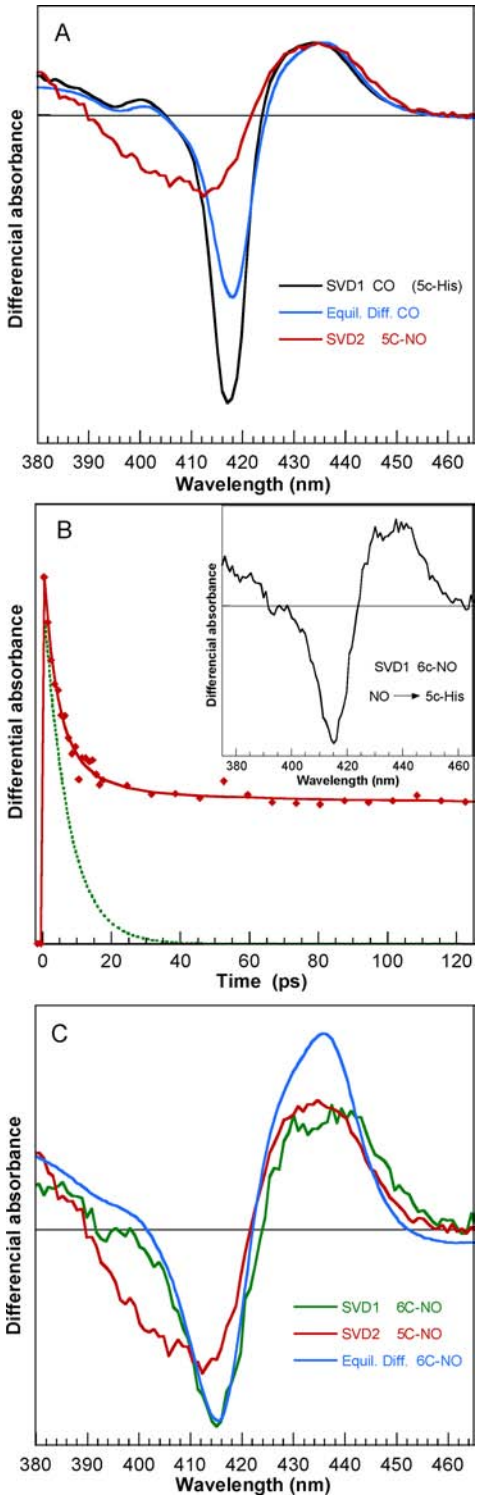

Figure 4. Comparison of the three ligation states of AXCP. (A) Equilibrium difference spectrum (blue) and normalized transient spectrum of 6c-CO (black) compared with the second component (SVD2) of 5c-NO (red). (B) Kinetics of NO rebinding to the 5c-His after dissociation of 6c-NO and associated transient spectrum (inset). The fitted parameters are τ_{ex} = 2 ps (excited states relaxation), τ_{gem6} = 52 ps, A_{gem6} = 43% (NO geminate rebinding), C = 57% (constant). The dotted curve is a 7-ps decay for comparison. (C) Equilibrium difference (blue) and normalized transient spectra (green) of 6c-NO compared with SVD2 spectra from the 5c-NO species (red).

exponentials in SVD2 kinetics have opposite signs (Figure 3B, inset), because 4c heme is disappearing while 5c-His is appearing with respect to the initial state (negative time delays). The induced absorption of SVD1 spectrum and the bleaching part of SVD2 spectrum (Figure 3A) represent the contribution of absorption spectrum of the 4c-heme. Consequenlty, we attempted to calculate the absolute absorption spectrum of the transient ferrous 4c-heme.

Spectrum of the 4-Coordinate Transient Ferrous Heme. At positive delays, each transient spectrum contains both the contribution of photodissociated 4c-heme, and nondissociated or reformed 5c-NO heme. This latter species is the only component before photodissociation, whereas the population of 4c-heme decreases with time. Therefore, the spectrum of the 4c ferrous heme was obtained by weighted subtraction of the spectrum of 5c-NO AXCP before photodissociation from the transient one measured at +10 ps. This procedure yields an uncertainty ~10% for the absorption and of ±2 nm for the position of the Soret maximum at 412 nm (Figure 3C). Interestingly, we observe two characteristics also seen in the spectrum of a ferric 4c-porphyrin model compound:[29] the Soret band of 4c-species is blue-shifted and has slightly higher absorption coefficient than that of the 5c-species. The blue shift is similar to that observed in the case of the ferrous 4c-protoheme (by ~16 nm) whose Soret maximum was measured at 415 nm.[30] Based on the transient resonance Raman spectra of photodissociated 5c-NO AXCP, we have previously proposed that the 4c AXCP transient heme is a high-spin species with single electron occupation of both d(z^2) and d(x^2-y^2) orbitals and with a slightly expanded porphyrin size relative to that of 5c-NO AXCP.[20]

Comparison with Other Coordination States. To ascertain the assignment of the transient SVD2 spectral component from 5c-NO AXCP, we compared it with transient SVD spectra from 6c-CO and 6c-NO species for which photodissociation generates only 5c-His AXCP and diatomic rebinding to 5c-His. Two SVD components were found in the case of NO dynamics, but only one for CO. Figure 4A compares the induced absorption part of the transient SVD1 spectral component corresponding to CO rebinding to 5c-His AXCP (bleaching at 417 nm and induced absorption centered at 435 nm) with the SVD2 spectral component from 5c-NO. Both induced absorptions centered at 435 nm are precisely overlapped each other, confirming the formation of 5c-His in the SDV2 from 5c-NO. The photodissociation of 6c-NO AXCP is analyzed in Figure 4B showing the kinetics of subsequent NO rebinding with the corresponding transient spectral component (inset). The rebinding of NO to the 5c-His heme appears slower (τ_{gem6} = 52 ps) than to the 4c-heme of AXCP with an amplitude of only 43% and a constant term representing 57% of NO which does not rebind in the picosecond time scale. The transient spectrum is clearly distinct from that of 5c-NO species with the minimum of bleaching due to dissociation of 6c-NO centered at 415 nm. This transient spectrum from 6c-NO is compared in Figure 4C with the 5c-NO SVD2 spectrum and with the static difference spectrum 5c-His − 6c-NO to illustrate that the second component (SVD2) in 5c-NO contains the 5c-His induced absorption and not the 6c-NO bleaching. The comparisons in Figure 4 thus provide a direct proof that in the case of 5c-NO photodissociation, the SVD2 component is neither attributable to 6c-NO nor to 5c-NO AXCP, but to the formation of 5c-His from 4c AXCP.

dx.doi.org/10.1021/ja312140f | J. Am. Chem. Soc. 2013, 135, 3248−3254

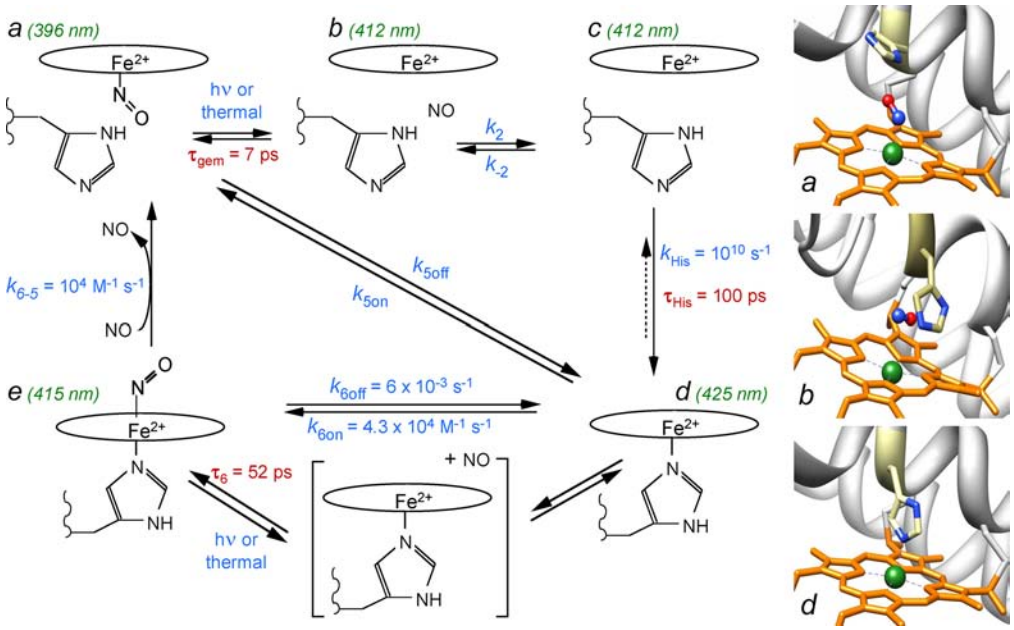

Figure 5. Dynamic model for NO interaction with ferrous AXCP. Photodissociation of NO is indicated by $h\nu$. NO release is also thermally driven. The Soret absorption maxima are indicated in green. The species are (a) 5c-NO AXCP with NO at the proximal side, which is the starting species of our experiments; (b) transient 4c-AXCP with NO dissociated and located within the heme pocket; (c) transient 4c-AXCP with NO located in the solvent; (d) 5c-His resting state AXCP; (e) 6c-His-NO AXCP. The rate constants (known values are indicated): k_1, thermal dissociation of NO; k_{gem}, rebinding rate; k_2 and k_{-2}, rates for exiting and accessing the heme pocket of the 4c-AXCP; k_{His}, rate for His rebinding after NO release (the shorter arrow indicates that the back process, albeit formally possible, has a low probability to occur and is not observed); k_{6on}, NO association rate from the solvent to 5c-His AXCP; k_{6off}, rate of NO dissociation of 6c-His-NO AXCP; k_{6-5}, rate of conversion of 6c-His-NO to 5c-NO AXCP; k_{5off}, overall dissociation rate of 5c-NO AXCP to the solvent; k_{5on}, overall association rate of NO from the solvent leading to proximal 5c-NO AXCP. Right panels: (*a*) equilibrium structure of 5c-His, (*b*) transient 4c AXCP at 10 ps after NO photodissociation, (*d*) proximal 5c-NO equilibrium structure. The structures *a* and *d* from Protein Data Bank are 2YLI and 2XLM. The structure *b* of transient 4c-heme AXCP was determined by molecular dynamics simulation performed with CHARMM.

DISCUSSION

Depending on the NO concentration, AXCP can form a distal 6c-NO species (low [NO]) or a proximal 5c-NO species (high [NO]). After NO dissociation from the proximal 5c-NO, NO geminately rebinds (~99%) with a rate of 1.4×10^{11} s^{-1}. From the dynamics of heme coordination, we have identified the rebinding of the proximal histidine with $k_{His} = 10^{10}$ s^{-1} rate which occurs for the fraction of 4c heme (~1%) to which NO does not rebind. Several consequences are directly inferred from these results. This large k_{His} value is a direct consequence of the high reactivity of the 4c-heme. Since NO within the heme pocket after its dissociation encounters numerous contacts with proximal His120, as calculated by simulated dynamics on a 50-ps time scale,[20] we infer that His rebinding occurs only after NO has left the heme pocket. Thus, *stricto sensu*, His rebinding does not compete with geminate NO rebinding but with direct binding of proximal NO from outside the heme pocket. Albeit formally possible, the Fe-His bond breaking of 5c-His does not occur without trans effect due to NO binding at the distal side. Consequently, the rate constant k_{-2} for NO rebinding from solution to the proximal side of the 4c heme is virtually equal to zero, which implies that NO released from the proximal pocket must rebind via the distal face.

The rebinding of His to 4c-heme is slower than that of proximal NO (k_{gem}), not because of the heme properties but likely because of constraints in the motion of His, (arising for example from the H-bond between His 120 and Asp121)[31] which should induce a small energy barrier. The appearance of the 5c-His species 100 ps after NO release precludes any proximal NO binding to 4c-heme from solution, consistent with His rebinding acting as a one-way gate for the release of proximal NO.

We may compare with other side-chains rebinding in 6c heme proteins. In absence of diatomic ligands, which may induce conformational changes, the endogenous sixth heme ligand distal methionine, when photodissociated from the bis-liganded 6c-heme (His, Met) rebinds to the 5c-His with time constants in the time range 5−35 ps in the cases of mitochondrial Cyt *c*[24] and oxygen sensor DOS.[32] We infer that His rebinding in AXCP appears slower, despite the higher reactivity of the 4c heme, not only because NO must be released from heme pocket first, but also because proximal His is stabilized in a noncoordinated conformation due to an H-bond with Asp121.[31] In contrast with AXCP, after release of the diatomic CO from the oxygen sensor DOS, the rebinding of the proximal methionine to 5c-His heme has been measured with a time constant of 100 μs,[32] remarkably slower by 6 orders of magnitude than for His rebinding in AXCP. The difference in these molecular dynamics may be due to the higher reactivity of the 4c-heme, but should also reside in the structural reorganization of the DOS protein, absent in the case of AXCP and for which only the rotation of the proximal side chain is necessary, whereas more pronounced changes occur in DOS.[33,34]

Finally, it must be noted that the rapid reattachment of the proximal His120 ligand to 4c heme means that subsequent heme-NO binding must begin on the opposite (vacant) distal face. Steric hindrance from the distal Leu16 residue

dx.doi.org/10.1021/ja312140f | J. Am. Chem. Soc. 2013, 135, 3248−3254

dramatically inhibits distal heme ligand affinity since its mere mutation (L16A) increases distal heme affinity for diatomic gas ligands by 6−8 orders of magnitude.[35,36] Thus, proximal and distal heme pockets work together to prevent irreversible binding of gases to the AXCP heme.

In conclusion, we identified the 4-coordinate heme of AXCP and the fast rebinding of proximal His in 100 ps, which functions as a one-way gate for NO release. The AXCP proximal His ligand controls distal versus proximal heme-NO coordination through two important ways: (1) the binding of one NO molecule to the distal side exerts a trans effect and cleaves the Fe-His bond, freeing the space for the binding of a second NO to the proximal side; (2) when NO leaves the proximal heme pocket, the proximal His rebinds, precluding proximal NO rebinding without a distal trans effect. This fast His rebinding process constitutes a kinetic trap mechanism, a unique property among heme proteins, different from the classical allostery of hemoglobin in which modification of the entire protein structure takes place.

AUTHOR INFORMATION

Corresponding Author

michel.negrerie@polytechnique.fr

Present Address

[§]Physical Biology Center for Ultrafast Science and Technology, Arthur Amos Noyes Laboratory of Chemical Physics, California Institute of Technology, Pasadena, CA

Notes

The authors declare no competing financial interest.

ACKNOWLEDGMENTS

We thank Fondation pour la Recherche Médicale for supporting our work with a fellowship attributed to B.-K.Y. C.R.A. acknowledges support from the National Science Foundation (Grant MCB-0745035) and assistance with protein preparation from Dr. Robert Eady.

REFERENCES

(1) Romão, M. J.; Archer, M. *Handbook of Metalloproteins*; John Wiley & Sons: Chichester, England, 2001; pp 44−54.

(2) Meyer, T. E.; Cheddar, G.; Bartsch, R. G.; Getzoff, E. D.; Cusanovich, M. A.; Tollin, G. *Biochemistry* **1986**, *25*, 1383−1390.

(3) Cross, R.; Aish, J.; Paston, S. J.; Poole, R. K.; Moir, J. W. B. *J. Bacteriol.* **2000**, *182*, 1442−1447.

(4) Cross, R.; Lloyd, D.; Poole, R. K.; Moir, J. W. B. *J. Bacteriol.* **2001**, *183*, 3050−3054.

(5) Mayburd, A. L.; Kassner, R. J. *Biochemistry* **2002**, *41*, 11582−11591.

(6) Choi, P. S.; Grigoryants, V. M.; Abruña, H. D.; Scholes, C. P.; Shapleigh, J. P. *J. Bacteriol.* **2005**, *187*, 4077−4085.

(7) Negrerie, M.; Bouzhir, L.; Martin, J.-L.; Liebl, U. *J. Biol. Chem.* **2001**, *276*, 46815−46821.

(8) Andrew, C. R.; George, S. J.; Lawson, D. M.; Eady, R. R. *Biochemistry* **2002**, *41*, 2353−2360.

(9) Lawson, D. M.; Stevenson, C. E. M.; Andrew, C. R.; Eady, R. *EMBO J.* **2000**, *19*, 5661−5671.

(10) Andrew, C. R.; Green, E. L.; Lawson, D. M.; Eady, R. R. *Biochemistry* **2001**, *40*, 4115−4122.

(11) Marti, M. A.; Capece, L.; Crespo, A.; Doctorovich, F.; Estrin, D. A. *J. Am. Chem. Soc.* **2005**, *127*, 7721−7728.

(12) Andrew, C. R.; Kemper, L. J.; Busche, T. L.; Tiwari, A. M.; Kecskes, M. C.; Stafford, J. M.; Croft, L. C.; Lu, S.; Moënne-Loccoz, P.; Huston, W.; Moir, J. W.; Eady, R. R. *Biochemistry* **2005**, *44*, 8664−8672.

(13) Nioche, P.; Berka, V.; Vipond, J.; Minton, N.; Tsai, A.-L.; Raman, C. S. *Science* **2004**, *306*, 1550−1553.

(14) Zhao, Y.; Brandish, P. E.; Ballou, D. P.; Marletta, M. A. *Proc. Natl. Acad. Sci. U.S.A.* **1999**, *96*, 14753−14758.

(15) George, S. J.; Andrew, C. R.; Lawson, D. M.; Thorneley, R. N. F.; Eady, R. R. *J. Am. Chem. Soc.* **2001**, *123*, 9683−9684.

(16) Martin, E.; Berka, V.; Sharina, I. G.; Tsai, A.-L. *Biochemistry* **2012**, *51*, 2737−2746.

(17) Petrich, J. W.; Lambry, J. C.; Kuczera, K.; Karplus, M.; Poyart, C.; Martin, J.-L. *Biochemistry* **1991**, *30*, 3975−3987.

(18) Gautier, C.; Negrerie, M.; Wang, Z. Q.; Lambry, J. C.; Stuehr, D. J.; Collin, F.; Martin, J.-L.; Slama-Schwok, A. *J. Biol. Chem.* **2004**, *279*, 4358−4365.

(19) Yoo, B.-K.; Lamarre, I.; Martin, J.-L.; Negrerie, M. *J. Biol. Chem.* **2012**, *287*, 6851−6859.

(20) Kruglik, S. G.; Lambry, J. C.; Cianetti, S.; Martin, J.-L.; Eady, R. R.; Andrew, C. R.; Negrerie, M. *J. Biol. Chem.* **2007**, *282*, 5053−5062.

(21) Andrew, C. R.; Rodgers, K. R.; Eady, R. R. *J. Am. Chem. Soc.* **2003**, *125*, 9548−9549.

(22) Ambler, R. P. *Biochem. J.* **1973**, *135*, 751−758.

(23) Norris, G. E.; Anderson, B. F.; Baker, E. N.; Rumball, S. V. *J. Mol. Biol.* **1979**, *135*, 309−312.

(24) Negrerie, M.; Cianetti, S.; Vos, M. H.; Martin, J.-L.; Kruglik, S. G. *J. Phys. Chem. B* **2006**, *110*, 12766−12781.

(25) Vandegriff, K. D.; Shrager, R. I. *Methods Enzymol.* **1994**, *232*, 460−485.

(26) Barbieri, S.; Murphy, L. M.; Sawers, R. G.; Eady, R. R.; Hasnain, S. S. *J. Biol. Inorg. Chem.* **2008**, *13*, 531−540.

(27) Negrerie, M.; Kruglik, S. G.; Lambry, J. C.; Vos, M. H.; Martin, J.-L.; Franzen, S. *J. Biol. Chem.* **2006**, *281*, 10389−10398.

(28) Petrich, J. W.; Poyart, C.; Martin, J.-L. *Biochemistry* **1988**, *27*, 4049−4060.

(29) Fang, M.; Wilson, S. R.; Suslick, K. S. *J. Am. Chem. Soc.* **2008**, *130*, 1134−1135.

(30) Arcovito, A.; Gianni, S.; Brunori, M.; Travaglini-Allocatelli, C.; Bellili, A. *J. Biol. Chem.* **2001**, *276*, 41073−41078.

(31) Hough, M. A.; Antonyuk, S. V.; Barbieri, S.; Rustage, N.; McKay, A. L.; Servid, A. E.; Eady, R. R.; Andrew, C. R.; Hasnain, S. S. *J. Mol. Biol.* **2011**, *405*, 395−409.

(32) Liebl, U.; Bouzhir-Sima, L.; Kiger, L.; Marden, M. C.; Lambry, J. C.; Negrerie, M.; Vos, M. H. *Biochemistry* **2003**, *42*, 6527−6535.

(33) Kurokawa, H.; Lee, D. S.; Watanabe, M.; Sagami, I.; Mikami, B.; Raman, C. S.; Shimizu, T. *J. Biol. Chem.* **2004**, *279*, 20186−20193.

(34) Park, H. J.; Suquet, C.; Satterlee, J. D.; Kang, C. H. *Biochemistry* **2004**, *43*, 2738−2746.

(35) Garton, M. E.; Pixton, D. A.; Petersen, C. A.; Eady, R. R.; Hasnain, S. S.; Andrew, C. R. *J. Am. Chem. Soc.* **2012**, *134*, 1461−1463.

(36) Antoyuk, S.; Rustage, N.; Petersen, C. A.; Arnst, J. L.; Heyes, D. J.; Sharma, R.; Berry, N. G.; Scrutton, N. S.; Eady, R. R.; Andrew, C. R.; Hasnain, S. S. *Proc. Natl. Acad. Sci. U.S.A.* **2011**, *108*, 15780−15785.